Journal of Electron Devices, Vol. 5, 2007, pp. 142-158

© JED [ISSN: 1682 -3427]

Journal of Electron Devices

Bridging the Gap between Nanoscopic and Macroscopic Properties: Case studies

Réda BENMOUNA*, Boumediène BENYOUCEF

Unité de Recherche ″Matériaux et Energies Renouvelables″

University Aboubekr Belkaïd, Faculty of Sciences, Department of Physics, Tlemcen

BP119, Algeria.

* To whom correspondence should be addressed

red_benmouna@mail.univ-tlemcen.dz

redabenmouna@yahoo.com

ABSTRACT

This paper deals with a broad topic entitled “Bridging the Gap between Nanoscopic and Macroscopic Properties” with a methodology based on specific examples. This is a broad subject involving a variety of techniques and properties. Establishing correlations between nanoscopic and macroscopic properties is an important and challenging problem. In this paper, we will briefly make a survey of what can be learned on the morphology and structure of composite materials, thermophysical properties and mechanical properties. We will show examples dealing with the case of PDLCs. We will also discuss other applications and in particular biological systems. One of the problems that we consider is how to correlate between the viscoelastic properties of soft biological materials (cells, membranes, hydrogels etc.) as measured by standard mechanical spectroscopy and nano mechanical mapping from newly developing techniques such as Atomic Force Microscopy (AFM) or Surface Force Apparatus (SFA). Another related question is how to relate measurements of the T_g of the materials under consideration using these and other more standard tools.

Keywords: nanoscopic, morphology, structure, thermophysical, microrheology, viscoelasticity, mapping.

1. INTRODUCTION

The subject of this paper is about bridging the gap between nanoscopic and macroscopic properties with some specific case studies. This is of course a very broad subject and we do not pretend to discuss it in detail. Only through few examples, we would like to show how one can obtain interesting and sometimes similar properties using completely different experimental tools. By exploring these properties on different scales of distances and times, one can get a detailed information on the structure and dynamics of the systems under investigation.

We will deal with different types of properties including morphology, structure, dynamic, thermophysical, microrheology, viscoelasticity and mapping. We will also consider entirely different systems by taking specific examples.

For example, we will give few examples of morphologies obtained by Polarized Optical Microscopy and Scanning Electron Microscopy of Polymer Dispersed Liquid Crystals (PDLCs) with different ranges of droplets sizes [1-5]. Depending on the initial system and the method of preparation, we obtained droplets dispersion in either the micrometer or nanometer size. These two cases lead to different applications. While the materials with micronsized droplets are characterized by strong scattering of light in the visible range, those with nanosized droplets do not scatter light but could lead to a strong phase shift and hence are very useful in optical fibers and spectral selectivity for telecommunication devices. This example gives a nice illustration for bridging the gap between micro and nanometer scale properties. But other examples will be considered from biology with entirely different physical phenomena and applications.

2. MORPHOLOGY

The examples of morphology considered here are obtained using essentially the Polarized Optical Microscopy (POM) and the Scanning Electron Microscopy (SEM) on Polymer Dispersed Liquid Crystals. These are composite materials based on mixtures of Polymer

and Liquid Crystals. They are characterized by a Swiss cheese morphology where the inclusions are filled with the low molecular weight Liquid Crystal molecules. Therefore, exploring the distribution of these inclusions and evaluating their sizes are crucial for their applications.

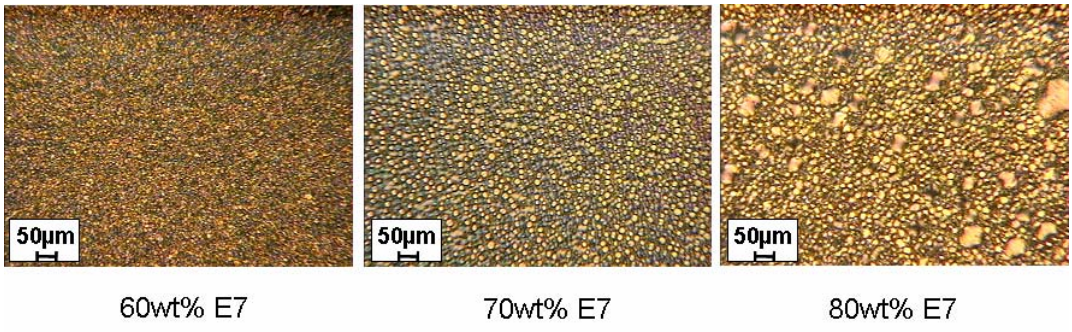

Figure 1: POM images of PDLCs showing micronsized droplets.

Figure 1 gives typical pictures obtained by POM on a system exhibiting micronsized droplets. Here we use the system made of the Optical Adhesive Norland (in short NOA) and the eutectic mixture of LCs known as E7. The composite material of the PDLC type is made by Polymerization Induced Phase Separation (PIPS) using UV light. This figure shows that the droplets diameter increases with the LC concentration and the distribution broadens.

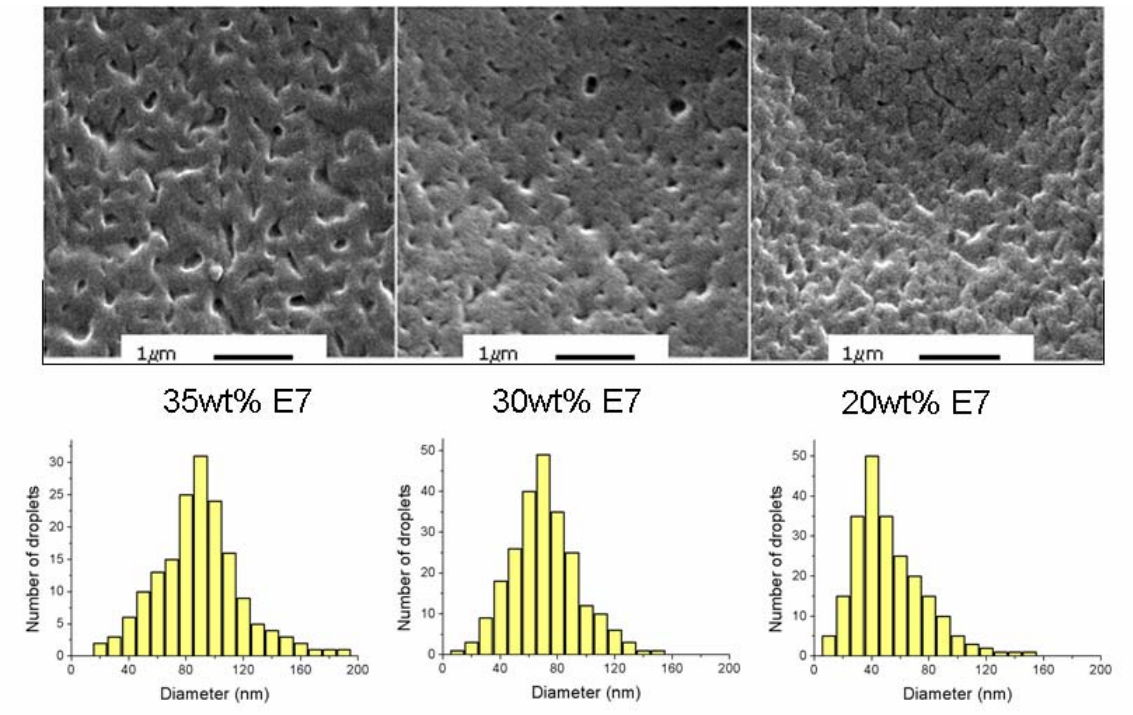

Figure 2: SEM images of PDLCs showing nanosized droplets and corresponding histograms of droplets diameter of thiol-ene / E7 at 3 concentrations of the LC.

In figure 2, we give typical electron micrographs obtained by SEM on the thiolene / E7 system. Under the same conditions of preparation and polymerization, changing the concentration of LC, one obtains these pictures accompanied with corresponding histograms. Effectively we have nanosized droplets. The droplets diameter increases with the LC concentration and the distribution broadens.

3. STRUCTURE

There are several experimental tools available for studying the structural properties of materials. Figure 3 illustrates the methods of analyzing the structure of composites in the direct space and in the corresponding reciprocal q space. This figure shows that the microscopy tools are useful in different space domains and the scattering techniques in the reciprocal q space $q \approx 1/r$.

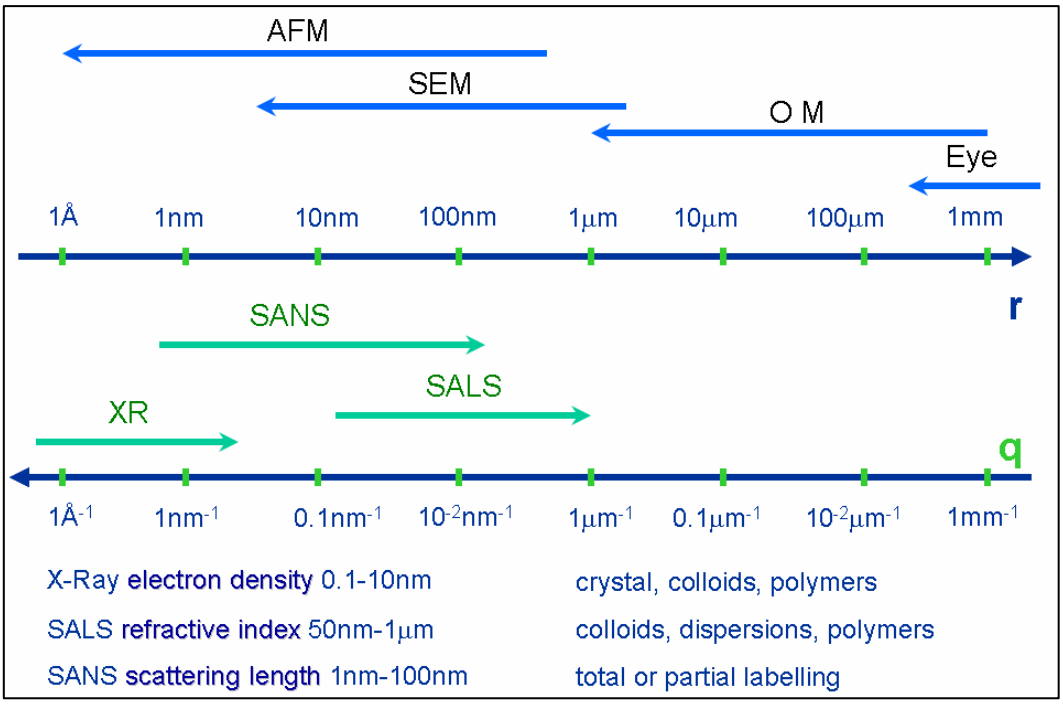

Figure 3: Microscopy and Scattering tools.

As one can see these tools cover a wide range from the nanometer to the macroscopic scale. Among the scattering techniques the most commonly used are: X-Rays, Light Scattering: Small or Wide Angle Light Scattering, Neutron Scattering: Small Angle Neutron Scattering (SANS) and Neutron Spin Echo: for Dynamic properties [6,7].

This figure shows the q windows where these techniques are operational together with some examples of the systems to which they are applicable.

The contrast in X-rays is provided by the number of electrons surrounding atoms, hence the larger the atom, the higher the contrast.

For light Scattering, the increment of refractive index of the polymer / solvent system $\frac{\partial n}{\partial c}$ (n=index of refraction, c concentration of polymer) provides the contrast.

For neutron scattering, the coherent scattering length (which is tabulated for each atom in particular hydrogen, Deuterium, Carbon, Oxygen) gives the contrast between molecular species in the system.

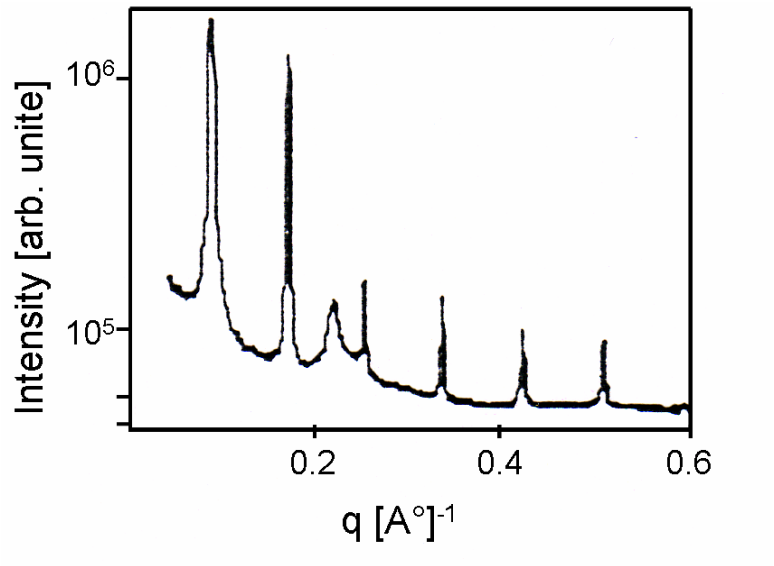

Figure 4: SAXS data of CL-DNA complexes showing six equidistant reflections and one additional broad reflection.

Figure 4 shows an example of an X-Ray spectrum obtained on the system DNA + lamellar phospholipid membrane [8,9]. It shows several peaks. The X-Ray peaks correspond to characteristic sizes of crystalline order in the complex DNA / Phospholipid membranes such as the lamella thickness, the inter distance between consecutive lamella and the distance between DNA molecules.

The second example dealing with the structural properties considers a mixture of DNA and Poly Ethylene Glycol (PEG) in an aqueous solution. This problem is interesting from the fundamental and applied points of view. Both polymers are miscible in water (hydrophilic) but they are characterized by a strong repulsion (incompatible). At a certain concentration of PEG, the DNA conformation undergoes a coil to globule transition (which is a first order transition). This means that there is a rapid transition from the swollen state (of DNA in water) to a collapsed state at a certain concentration of PEG as shown in figure 5. Changes of conformation of the DNA molecules at different concentrations of PEG from zero (absence of PEG and binary DNA / water solution) to the concentration of the coil → globule transition are important to evaluate. A possible way to solve this problem is to use static and dynamic light scattering.

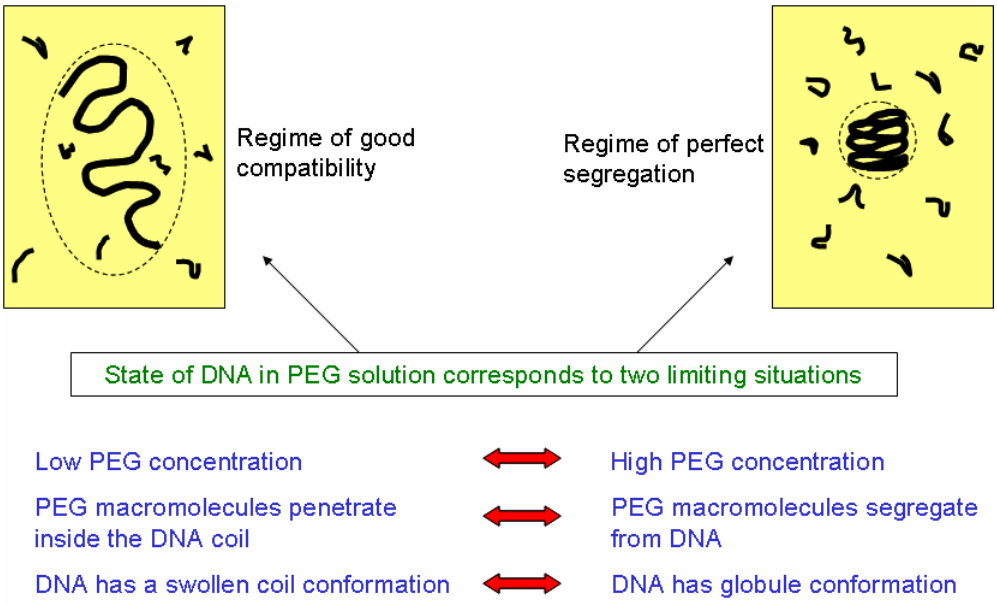

Figure 5: Condensation of DNA in solution of polyethylene glycol (PEG).

A Zimm plot analysis of the light scattering from this system yields the radius of gyration of DNA R_g, the second virial coefficient A_2 and the weight average molecular weight M_w [10]. This plot is shown in figure 6.

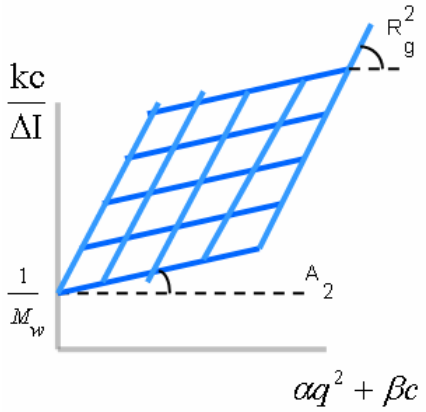

Figure 6: Zimm plot analysis of the light scattering, α and β are adjustable parameters.

The slope of the $q = 0$ curve gives A_2 while the slope of $c = 0$ yields R_g according to the standard formula

$$\frac{kc}{\Delta I} = \frac{1}{M_W}(1 + \frac{1}{3}q^2 R_g^2) + 2A_2 C \qquad (1)$$

where k is a constant characteristic of the experimental set up and ΔI the scattered intensity. The three parameters M_w, R_g, A_2 are systematically extracted from the Zimm plot analysis. The radius of gyration describes de degree of swelling of the DNA chain while the second virial coefficient describes the quality of solvent (A_2 is high and positive for good solvent, A typical value is $A_2 = 2.10^{-4}$ cm^3/g^2).

Adding PEG by a small amount and performing a similar Zimm plot analysis yields different values of R_g and A_2 while M_w should remain constant.

One may assume that PEG only changes the solvent quality and consider a quasi-binary DNA / solvent system.

A more rigorous analysis using theories of ternary polymer solutions is possible but not needed for preliminary studies. One expects that R_g and A_2 decrease dramatically as the concentration of PEG approaches the limit of coil to globule transition of DNA. The plot of R_g and A_2 versus PEG concentration should give the scaling result R_g scales as

$$Rg = M_W^{\nu} \qquad (2)$$

where the exponent ν vary from ν=0.6=3/5 (good solvent) to ν=0.33=1/3 (collapsed state).

A similar investigation can be made using Quasi Elastic Light Scattering of this system. Here on measures the field correlation function g(q,t) as a function of time fixing the value of q or scattering angle. The field correlation function g(q,t) is related to the intensity auto-correlation function $G^{(2)}$ by Siegert formula

$$G^2(q,t) = 1 + \beta \mid g(q,t) \mid^2 \qquad (3)$$

where β is a constant characteristic of the experimental set-up and is of the order of 1. The time decay of g(q ,t) should be a simple exponential decay of the form

$$g(q,t) \approx e^{-Dq^2 t} \approx e^{-t/\tau_q} \qquad (4)$$

where τ_q is the relaxation time $\tau_q = 1/Dq^2$ and D is the diffusion coefficient. The latter is related to the viscosity of the solution η and the hydrodynamic radius of DNA chains as

$$D = \frac{k_B T}{6\pi\eta R_H} \quad (5)$$

One may determine D and R_H as a function of the concentration of PEG under similar condition as R_g. It would be interesting to have the ratio R_H / R_g and the critical exponent

$$R_H \approx M_W^{\nu} \quad (6)$$

ν should have similar asymptotic values as the exponent in R_g.

If the field correlation function has a more subtle decay such as a bimodal or a stretched exponential one can perform such a detailed dynamical analysis using available appropriate models.

4. THERMOPHYSICAL

In this paragraph, we consider properties related with the miscibility of different constituents in the mixture and the phase diagrams [11,12].

DSC measurements give the transition temperatures and the enthalpy exchange during phase transitions. We are particularly interested on the glass transition temperature T_g and order disorder transitions such as nematic to isotropic transition for liquid crystals.

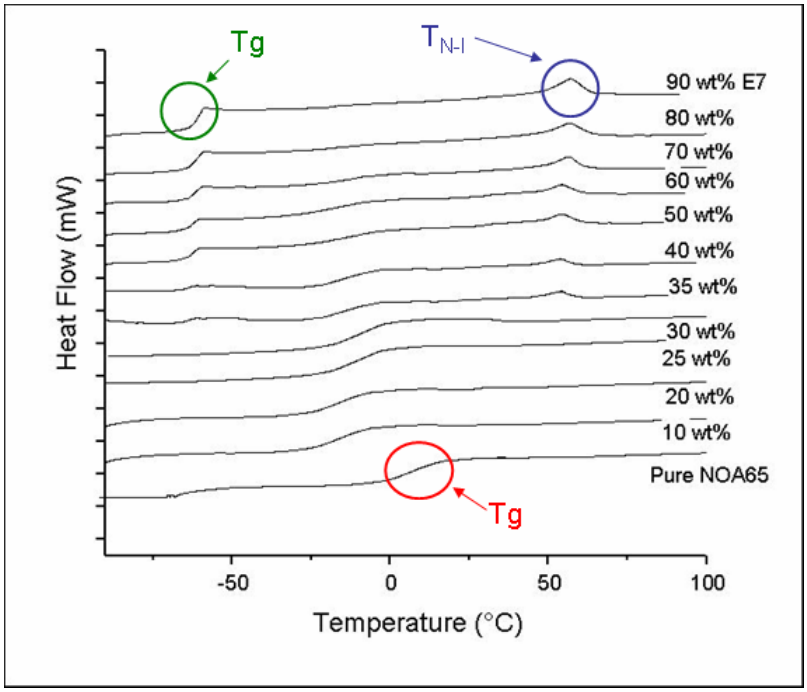

Figure 7: DSC thermograms for mixture of E7 and NOA65.

Figure 7 gives the thermograms for NOA / E7 at different concentrations of the LC. We see clearly the glass transition of NOA and T_{NI} of E7 and their variations when the LC concentration increases. The glass transition is an important property that can also be determined by looking at the variation of tangent loss angle $\tan\delta = \frac{G''}{G'}$ obtained from Dynamic Mechanical Analysis, where G` and G`` are the elastic (storage) and loss moduli of the sample under investigation. This aspect will be examined in the following paragraph.

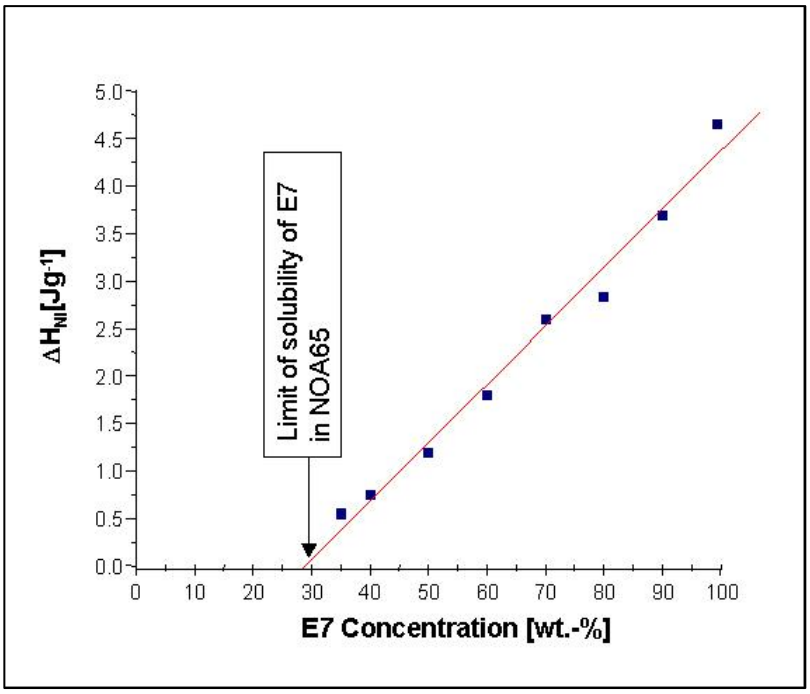

Figure 8: Enthalpy change at the nematic to isotropic transition.

From the curve of ΔH_{NI} versus LC concentration, one can obtain both the limit of solubility at the intersection with the x-axis and the amount of LC dissolved in the polymer matrix. This amount reduces drastically the T_g of Polymer weakening its mechanical strength.

Comparison of T_g from DSC and DMA is an interesting aspect, which could be addressed considering either PDLC systems or biological systems. Another interesting property is the surface T_g compared with the bulk T_g. The former was recently investigated using Atomic Force Microscopy (AFM).

5. MICRORHEOLOGY and VISCOELESTICITY

Biological systems have known a renewed interest in the light of new developments of materials with nanostructures.

Figure 9 shows an electron micrograph of actin bundles (fibres) that are responsible for the viscoelastic response of cells (muscles for example) [13]. These are huge molecules with an end–to-end distance of several 100μm, quite rigid since the persistence length is

about 17μm. They are thin filaments of diameter 0.01μm. A strong overlap of chains is found even at low concentrations.

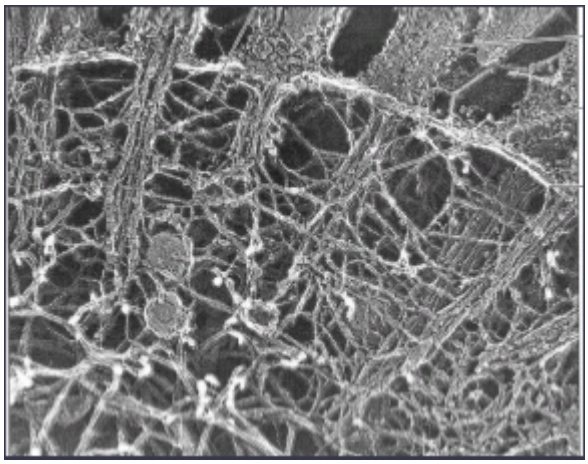

Figure 9: Electron micrograph of the cytoskeleton of an intestinal epithelial cell near the plasma membrane, showing networks and bundles of actin and accessory proteins.

Investigations of the viscoelastic parameters of systems such as Actin network and Polyacrylamide in water were reported using the Brownian motion of a micronsized sphere and laser interferometry technique. Similar studies might be under-taken using Confocal Fluorescence Microscopy. The problem is as follows. Assume we have a spherical bead of radius R embedded in a polymer network of a certain mesh size. If one can develop a technique to measure the mean square displacement of the bead $<|\Delta r|^2>$ then it would be possible to infer the viscoelastic parameters G` and G`` using linear response theory results.

The following figure shows the three cases of a viscous medium, elastic medium and visco-elastic medium. There is a characteristic time $\tau=\eta/G$ (η being the viscosity and G the elastic modulus) separating the viscosity regime at shorter times and elastic regime at longer times as shown in this figure.

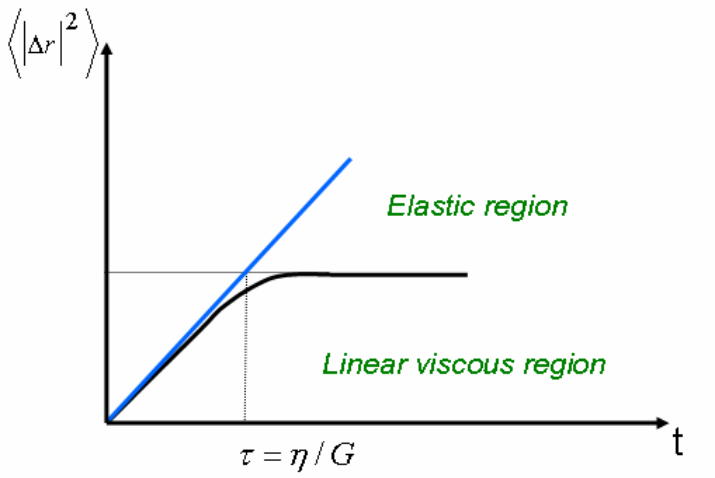

Figure 10: Curve of a viscoelastic medium.

Note that the bead diffusion coefficient is related to the mean square displacement by the formula first derived by Einstein $<|\Delta r|^2>=6Dt$, where t is the time and D the diffusion coefficient. The viscoelastic parameters G`(ω) and G``(ω) are obtained according to linear response theory using the following procedure.

Suppose one knows $<|\Delta r|^2>$ from the experiment. This is just the square distance between the original position of the bead and its position at time t. Then one can determine the imaginary part of the quantity

$$\alpha(\omega) = \alpha'(\omega) + i\alpha''(\omega) \tag{7}$$

using the linear response theory result [13]

$$<|\Delta r|^2>= \frac{4k_B T\alpha''(\omega)}{\omega} \tag{8}$$

The real part can be deduced from the Kramers-Kroenig relations

$$\alpha'(\omega) = \frac{2}{\pi} P\int_0^\infty du \frac{u\alpha''(\omega)}{u^2 - \omega^2} \tag{9}$$

where P is the Principle Part of the Integral.

This is a standard procedure when one is dealing with complex physical quantities. Knowing the real and imaginary parts, one can determine α(ω) completely from which one gets the real and imaginary parts G`(ω) and G``(ω) of G(ω) by using

$$G(\omega) = \frac{1}{6\pi R\,\alpha(\omega)} \qquad (10)$$

where R is the radius of the probe Brownian particle.

A typical plot of G` and G`` for a viscoelastic fluid is shown in figure 11. At low frequencies, one has the viscous flow behavior whereby G`(ω) goes to 0. Since the reptation regime is extremely slow, it may not be accessible by standard methods. In the intermediate frequency range, one has the rubbery plateau whereby G`(ω) is independent of ω and in the high frequency regime, one finds the scaling behavior $G`(\omega)\approx\omega^{Z}$ and $G``(\omega)\approx\omega^{Z}$.

The exponent Z is interesting because it yields information on the dynamical relaxation of chains. For example, the Rouse model would give Z=1/2 while another dynamical mechanism would lead to a different exponent.

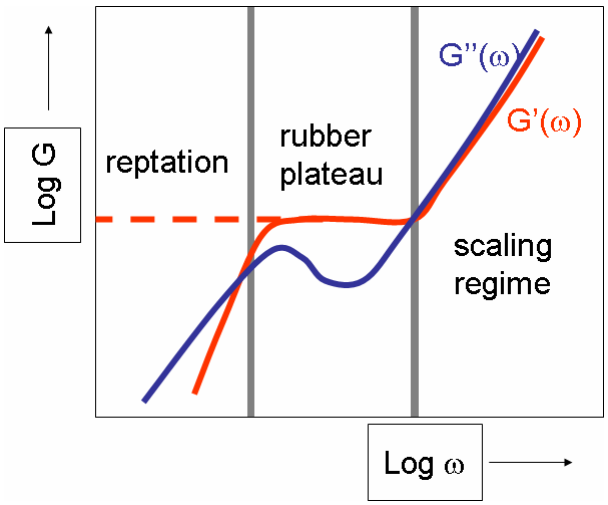

Figure 11: Viscoelastic parameter for a viscoelastic material.

It is worth noting that as the bead radius R increases, the frequency where G` and G`` meet, shift to lower values. For a bead radius higher than half the mesh size of the

polymer network, one probes the collective dynamics of the network. The probe particle experiences the contraction and expansion of the network as a whole. For a radius smaller than half the mesh size, one probes the local dynamics since the particle can easily go from one site to another. Similar measurements with confocal Microscopy could be used to determine the properties of biological materials.

Another problem is related to the AFM method used to map the T_g (microcalorimetry) the roughness (morphology) and the viscoelastic properties of biological materials.

Measurements of surface T_g and bulk T_g give detailed thermophysical analysis which could be compared with the results of DSC. Figure 12 describes the basic principle behind the AFM technique [14,15]. The tip at the end of the cantilever undergoes a deflection at the contact of the sample. This deflection is measured with a photodiode that records the reflected laser beam. The piezo scanner controls the position of the cantilever and is programmed according to the mode of functioning of the AFM apparatus (scanning mode, tapping mode etc.). One of the basis properties measured by the AFM technique is the force distance curve since one can record the force felt by the cantilever at the contact with sample or even when there is indentation (penetration) of soft deformable samples such as polymer systems.

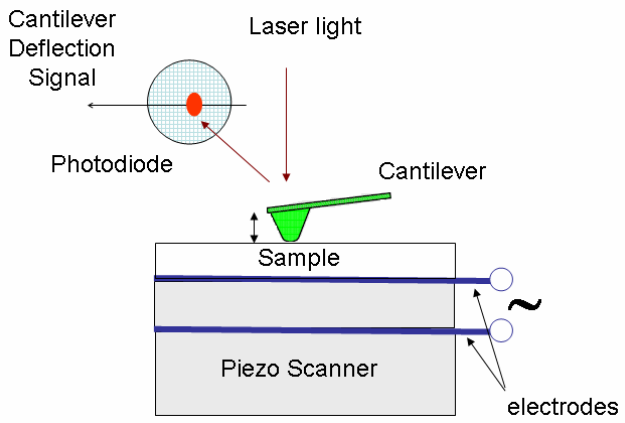

Figure 12: Principle of Atomic Force Microscopy (AFM)

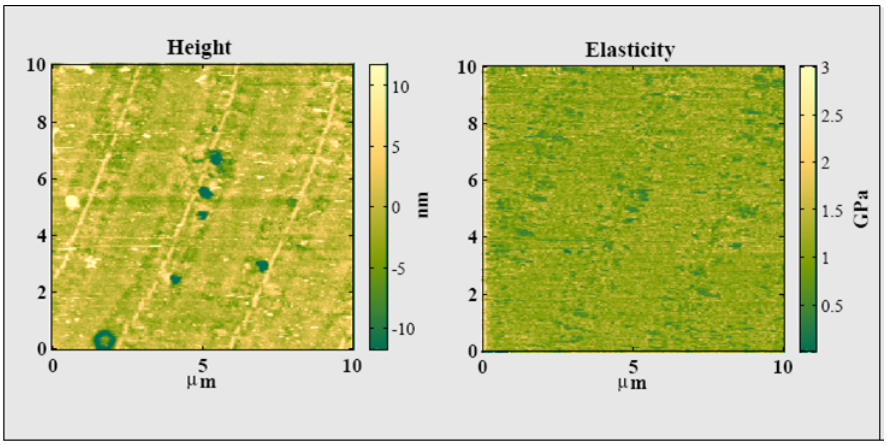

Figure 13: Elasticity mapping of the roughness of biological systems using AFM.

A typical example of the roughness and the micro mechanical mapping of biological systems using AFM is given in Figure 13. This is an interesting example that could be used for various biological systems such as membranes, cells, proteins or others.

Therefore, systems having different elastic properties could be characterized quite nicely with the mapping procedure as shown in this figure [16].

This paper gives a broader view of the research possibilities and opens up new perspectives for the future.

6. CONCLUSION

From the few examples considered here above, we scanned a subject which is broad, diverse, rich and at the same time quite complex and exciting. It is clear that a uniform description is not yet possible since the systems examined are so different. The common feature is the dimensionality, the range of correlations in the system and the time scales describing the dynamical behavior. However, the experimental techniques that are in constant development can be applied to this or that system and examples taken to illustrate the phenomena under investigation. We hope that, by briefly discussing different aspects, we have contributed in advancing the understanding of the importance of scales in space and time in various systems from biology, physics and chemistry.

REFERENCES

[1] P. S. Drzaic, *Liquid Crystal Dispersions*, World Scientific, Singapore, 1995.

[2] J. W. Doane, *Polymer Dispersed Liquid Crystals displays*, World Scientific, Singapore, 1990.

[3] R. Benmouna, V. Rachet, P. le Barny, P. Feneyrou, U. Maschke, X. Coqueret, *J. Polym. Eng.*, 26(5), 499, 2006.

[4] R. Benmouna, V. Rachet, P. le Barny, P. Feneyrou, U. Maschke, X. Coqueret, *J. Polym. Eng.*, 26(7), 655, 2006.

[5] L. Benkhaled, R. Benmouna, X. Coqueret, U. Maschke, F. Z. Abdoune, A. Berrayah, L. Méchernène, *Mol. Cryst. Liq. Cryst.*, 412, 1087, 2004.

[6] B. Berne, R. Decora, *Dynamic Light Scattering: Applications to Biologie*, Academic Press, New York, 1976.

[7] J. Higgins, H. Benoît, *Polymers and Neutron Scattering*, Oxford University Press, Oxford, 1994.

[8] J.O. Rädler, I. Koltover, T. Salditt, C.R. Safinya, *Science*, 275, 810, 1997.

[9] R. Podgornik, H.H. Strey, V.A. Parsegian, *Physical forces molding DNA-lipid complexes, in "Gene Therapy: Therapeutic Mechanisms and Strategies"*, Eds., New York, 209, 2000.

[10] H. Yamakawa, *Introduction to Polymer Solutions*, Harper & Row, Chicago, 1970.

[11] P.J. Flory, *Principles of Polymer Chemistry*, Cornell University Press, Ithaca, 1965.

[12] P.G. de Gennes, *Modern Concepts of Polymer Physics*, Cornell University Press, Ithaca, 1979.

[13] B. Schnurr, F. Gittes, F.C. Mackintosh, C.F. Schmidt, *Macromolecules*, 30, 7781, 1997.

[14] H. J. Butt, *Biophys. J.*, 60, 1438, 1991.

[15] S. A. Soomro, R. Benmouna, R. Berger, H. Meier, *Eur. J. Org. Chem.*, 16, 3586, 2005.

[16] B.B. Akhrimetchev, H. Brown, J. Bemis, G.C. Walker, Poster presented at 43rd Annual Biophysical Society Meeting, 2003.